

Identification of Peptide Ligands for Target RNA Structures Derived from the HIV-1 Packaging Signal ψ by Screening Phage-Displayed Peptide Libraries

Anette Pustowka,^[a] Julia Dietz,^[a] Jan Ferner,^[b] Michael Baumann,^[b] Margot Landersz,^[a] Christoph Königs,^[a] Harald Schwalbe,^[b] and Ursula Dietrich^{*[a]}

RNA molecules have the capacity to adopt complex three-dimensional structures, which allow specific recognition of proteins or RNA ligands. This property enables RNA molecules to perform essential regulatory and catalytic functions in the cell; these include modulation of gene activities, RNA transport, protein biosynthesis, splicing, viral genome packaging, and many more.^[1] Consequently, RNA molecules have also become an attractive target for therapeutic interventions, especially since sequence information of the human genome combined with modern chip technologies allows the association of defined RNA molecules with specific pathological alterations.

RNA molecules mostly exert their regulatory functions by specific interactions with proteins. Clearly, posttranscriptional base modifications play an important role in protein recognition, as shown for the specific interaction of tRNA molecules with aminoacyl-tRNA synthetases.^[2] In the last few years, however, X-ray crystallography and NMR spectroscopy have provided additional insights into some rules governing specific RNA–protein recognition.^[3] According to these analyses, structural features of RNA molecules like A-form helices, single-stranded loops of a hairpin, or bulged regions are also important elements for protein recognition.^[4] Arginine-rich motifs bind to RNA structures by adopting different conformations within different complexes.^[5] Other specific contacts between single-stranded RNA loops and proteins are often mediated by aromatic amino acids. In any case, induced fit of either one or both binding partners is very frequently observed in RNA–protein recognition and is mechanistically important for biological regulation.^[6–9]

In terms of therapeutic interventions, one approach to identify molecules that interfere with specific RNA–protein interactions is to select those molecules from complex chemical or molecular

libraries. The huge structural space of RNA phenotypes is exploited in screening procedures in which RNA aptamers are selected and amplified over multiple rounds as the best-fitting ligands for a target molecule. The name SELEX (systemic evolution of ligands by exponential enrichment) has been coined for this procedure.^[10] Other approaches use a given RNA structure as a target to select for specific ligands from compound libraries.^[11, 12]

Phage-displayed peptide libraries have been widely used to select peptide ligands for antibodies, protein domains, or peptides.^[13] Since the selection of peptide ligands is based on the structural recognition of the peptide motifs presented at the phage surface, phage-display technology should also be suited for the selection of peptide ligands for RNA structures. In fact, some groups have already used phage-display technology for this purpose: the U1 small nuclear RNA has been a target to select proteins or antibody binding fragments (Fab) from phage libraries.^[14–17] Tailored phage libraries expressing zinc finger motifs or arginine-rich motifs were generated to select protein domains binding to the Rev responsive element stem-loop IIB (RRE-IIB) from HIV-1 and the 5S rRNA^[18, 19] or the Tat transactivating region (TAR).^[20, 21]

The aim of this study was to select specific peptide ligands for the RNA packaging structure ψ (ψ) of HIV-1. The ψ RNA is a highly structured region located at the 5'-untranslated end of unspliced HIV-1 RNA molecules. The ψ RNA is responsible for specific encapsidation of two viral RNA genomes into the virions during their assembly process at the plasma membrane.^[22] Specific recognition of viral genomic RNAs is mediated by the interaction of the ψ RNA with the viral Gag polyprotein, in particular, with the nucleocapsid protein NCp7 containing two zinc fingers.^[23, 24] The entire ψ region consists of about 120 nucleotides predicted to form four individual stem-loop structures, SL1–SL4 (Figure 1). Several additional functions are also located within the ψ structure like the dimerization sequence (DIS) in SL1, the splice donor site (SD) in SL2, and the Gag initiation codon preceding SL4. Although all four stem-loops are involved in the RNA encapsidation process, SL3 is the major packaging signal, as it is capable of direct packaging of heterologous RNAs into virus-like particles.^[25] A number of NMR studies have proven the specific interaction of SL3, and also of the other SL structures, with the NCp7 protein.^[26–28] The key structural determinants are interactions between aromatic residues of the zinc fingers and the SL3 RNA sequence.^[29–31] A detailed study combining biochemical analysis and NMR spectroscopy of SL3 has shown the specific interaction of full-length Gag with the GGAG tetraloop as well as with a purine-rich internal loop of SL3.^[32] Furthermore, Gag binding and polymerization leads to progressive unwinding of the SL3 secondary structure.^[33] As packaging of viral RNA genomes into virions is an essential step in the viral replication cycle, this process should also be suited for antiviral interventions. In fact, antisense RNA directed against the ψ region and inhibitors for the zinc finger protein NCp7 have shown antiviral activity.^[34, 35] Our approach focuses on the selection of peptide ligands from phage-displayed peptide libraries, which specifically bind to the complete ψ RNA or to single stem-loops thereof.

[a] Dr. U. Dietrich, A. Pustowka, J. Dietz, M. Landersz, C. Königs
Georg-Speyer-Haus
Institute for Biomedical Research
Paul-Ehrlich-Strasse 42–44
60596 Frankfurt (Germany)
Fax: (+49) 69-63395-297
E-mail: ursula.dietrich@em.uni-frankfurt.de

[b] J. Ferner, Dr. M. Baumann, Prof. Dr. H. Schwalbe
Institute for Organic Chemistry and Chemical Biology
Center for Biomolecular Magnetic Resonance
Johann Wolfgang Goethe University
Marie-Curie-Strasse 11, 60439 Frankfurt am Main (Germany)

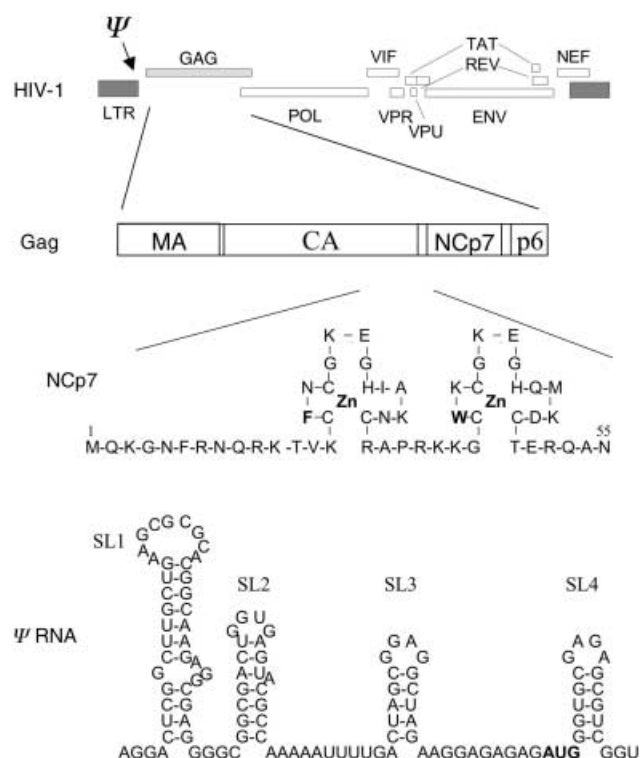


Figure 1. Location of the packaging signal ψ and the gag gene within the HIV-1 genome. The nucleocapsid protein NCp7 of the Gag polyprotein interacts through its zinc fingers (zinc in bold) with the ψ -RNA structure and in particular with the third stem-loop SL3. The Gag initiation codon is shown in bold.

Immobilized full-length in vitro transcribed ψ RNA was stable under screening conditions and was in a conformation that would allow binding of the natural ligand, HIV-1 Gag protein p55. Full-length ψ RNA and short synthetic RNA molecules representing stem-loops SL1, SL2, and SL3 were used as the

targets in the biopanning rounds. For negative selections, we used an unrelated RNA of similar size (CCR5) or mutated stem-loop RNAs. After several rounds of positive and negative selections, phages were analyzed for specific binding to the target RNAs derived from the ψ region by ELISA. Between 8.3 and 19.8% of the phage clones were positive depending on the library used. Peptide motifs of specific phages were identified by sequencing the genome inserts encoding them. Among the most prominent motifs selected was a cluster of aromatic amino acids in conjunction with positively charged amino acids. Interestingly, similar aromatic motifs could be selected with full-length ψ RNA and with the single stem-loop RNAs (all or SL1, SL2, and SL3; Table 1).

The specificity of the corresponding phage for the ψ RNA and the stem-loops SL1, SL2, and SL3 was confirmed by ELISA (Figure 2). Specific binding of the phage to full-length ψ RNA was

Table 1. Aromatic peptide motifs selected with RNA structures derived from the HIV-1 packaging signal ψ .

Phage clones	Target RNA	Peptide motifs
12.3/12.9/12.18	ψ	HHSWHWWHQDRQ
12.21	ψ	RWWSWPSYTQSS
12.25	ψ	WPMTNWFHYHSW
12.55	ψ	HFWPWWLYSGTW
7.5	ψ	HWWLFWW
7c.47	ψ	HWPFLLHS
12.64	SL1	HWWPYHTSTSQP
D4E12.7	SL1	FPWHFHRAPSIH
A557C.64/82/95	SL1	HWWSRHH
7C.8/7C.56	SL2	HWWSRHH
C.7x	SL1	SPWHPHR
A557C.41	SL2	HPHWWHR
A557C.122	SL2	HWWNYRH
A557C.156	SL2	HWWSWRH
A557C.166	SL2	HQHWKWR
C5E7.12.64	SL3	IPWTQHMAMSPM

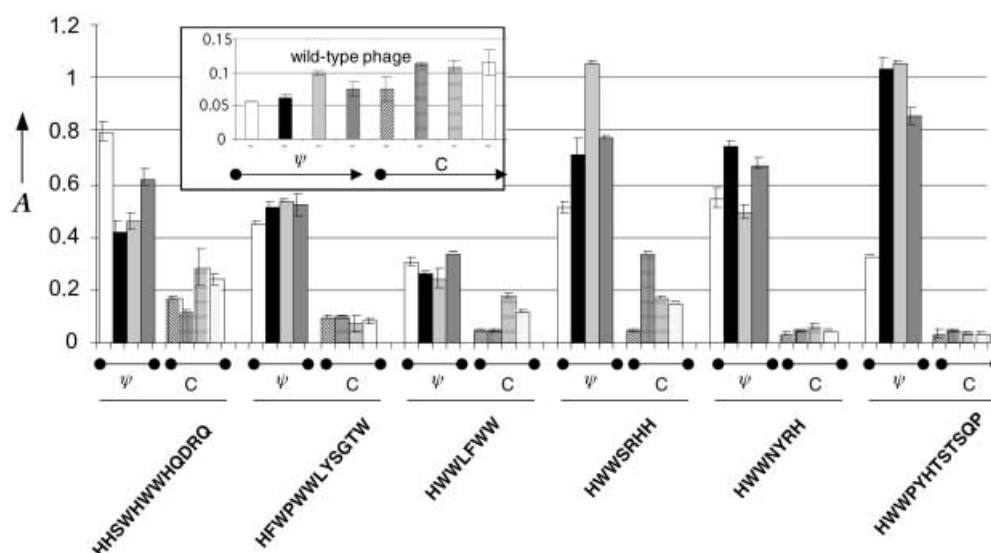


Figure 2. Analysis by ELISA of binding of phages selected with RNAs derived from the ψ region after several rounds of positive and negative selection to ψ RNAs (ψ : full-length ψ RNA, white bars; SL1, black bars; SL2, light grey bars; SL3, dark grey bars) and control RNAs (C: CCR5-RNA, diagonal stripes; mutated SL1, grids; mutated SL2, horizontal stripes; mutated SL3, dots). The insert graph shows binding of wild-type phages to the same RNAs. The optical density values (A) are the mean of triplicate measurements at 492 nm.

also visualized by band-shift analysis by separation on polyacrylamide gels (Figure 3). Specific binding of the hydrophobic peptide motifs to ψ RNA was confirmed for synthetic peptides corresponding to the peptide sequences on the selected phages by ELISA (data not shown) and CD spectroscopy (Figure 4). After Boltzmann transformation ($y = (A_1 - A_2)/(1 + e^{(x-x_0)/dx}) + A_2$; fitting the data asymptotically to the initial value with no peptide (A_1), to the final value with a large excess of peptide (A_2), and to the value and the slope of the inflection point x_0 which corresponds to the binding constant, K_D), the deduced affinity of a consensus peptide HWWPWW for ψ RNA was $25 \pm 2 \mu\text{M}$ and for SL3 was $34 \pm 2 \mu\text{M}$. Exchange of single amino acids within the HWWPWW peptide for alanine

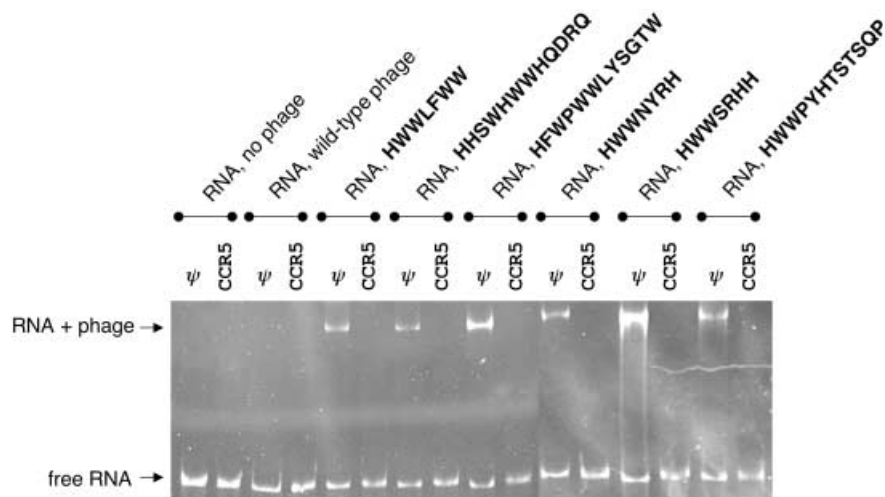


Figure 3. Analysis of binding of phages selected with RNAs derived from the ψ region after several rounds of positive and negative selection to full-length ψ RNA and CCR5 control RNA by band-shift analysis. Specific band shifts are observed for the selected phages in the presence of ψ RNA.

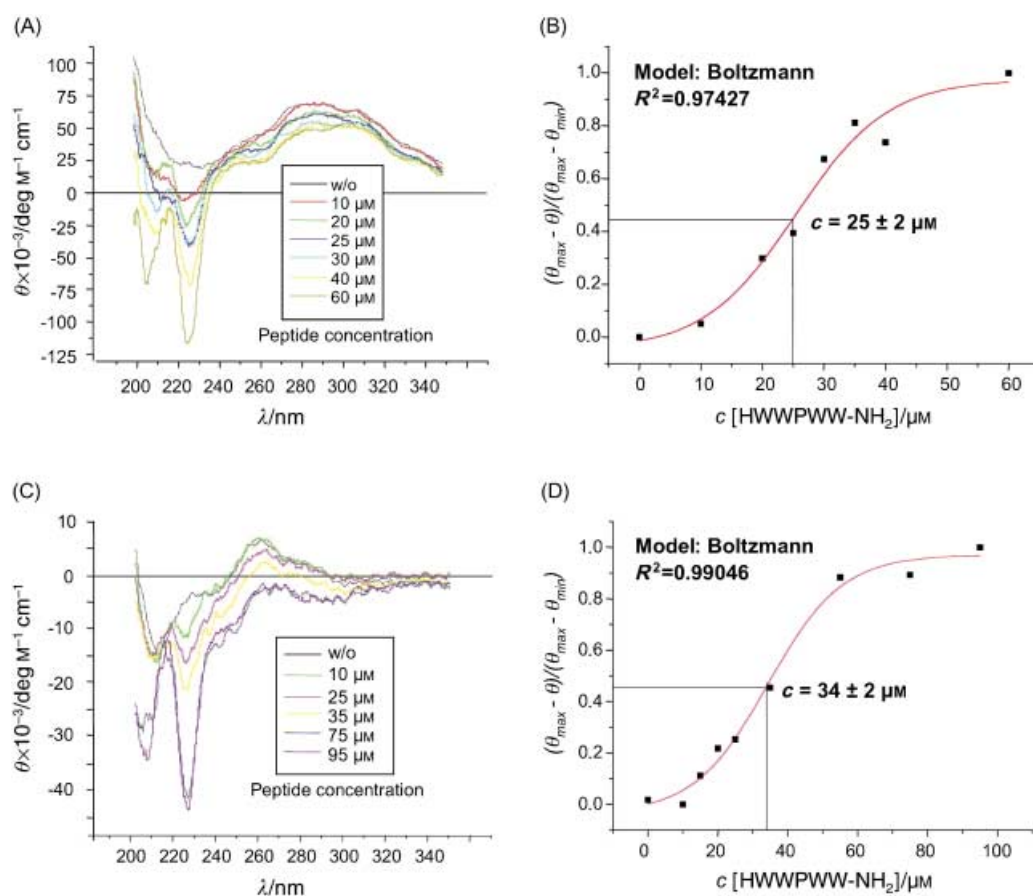


Figure 4. Detection of binding between peptide HWWPWW-NH₂ and ψ RNA (A and B) and stem-loop SL3 (C and D) by CD spectroscopy. A) CD spectra (at 20 °C) show the decrease of the positive molar ellipticity at around 290 nm which stems from the secondary structure of the ψ RNA (0.2 μM) induced by titration with the peptide HWWPWW-NH₂ in 100 mM potassium phosphate buffer (pH 6.5). B) Plot of the molar ellipticity decrease at 290 nm ($\theta_{\text{max}} - \theta$) in relation to the maximum decrease ($\theta_{\text{max}} - \theta_{\text{min}}$) against the peptide concentration. θ_{max} is the maximum molar ellipticity at 290 nm during the experiment and θ_{min} is the minimum value. Curve fitting assumed the sigmoidal Boltzmann function ($y = (A_1 - A_2)/(1 + e^{(x-x_0)/dx}) + A_2$) and resulted in a binding constant K_D of $25 \pm 2 \mu\text{M}$. C) CD spectra (at 20 °C) show the decrease of the positive molar ellipticity around 260 nm which stems from the secondary structure of the SL3 RNA (0.7 μM) induced by titration with the peptide HWWPWW-NH₂ in 100 mM potassium phosphate buffer (pH 6.5). D) Plot of the molar ellipticity decrease at 260 nm ($\theta_{\text{max}} - \theta$) in relation to the maximum decrease ($\theta_{\text{max}} - \theta_{\text{min}}$) against the peptide concentration. θ_{max} is the maximum molar ellipticity at 260 nm during the experiment and θ_{min} is the minimum value. Curve fitting assumed the sigmoidal Boltzmann function (as above) and resulted in a binding constant K_D of $34 \pm 2 \mu\text{M}$.

was followed by CD spectroscopy and showed residues H1, W3, and W5 to be important for RNA binding; in contrast, mutation of W2 and P4 resulted in improved RNA binding.

Tryptophan motifs are known to be important for RNA binding. NMR analysis of SL3 RNA with the nucleocapsid protein NCp7 showed the specific stacking interaction of W37 of the second zinc finger of NCp7 with unpaired guanosine residues (especially G318) within the SL3 tetraloop.^[36, 37] NCp7 also binds to the single-stranded loops of SL1, SL2, and SL4 with affinities of 20–140 nM.^[38] High-resolution structures revealed similar interactions between NCp7 and the different stem-loops involving the hydrophobic cleft of the zinc fingers and unpaired guanosine residues. In fact, this stacking interaction was used in binding assays to study the affinities of wild-type and mutated stem-loops SL1–SL4 for NCp7, based on the quenching of the fluorescence of W37 by guanosine residues in the single-stranded loops of SL1–SL4.^[32, 38] Interestingly, we also selected similar tryptophan-containing peptide motifs independently of which RNA was used as the target. Furthermore, we could confirm specific binding of the hydrophobic peptides to ψ RNA as well as to SL1, SL2, and SL3 by ELISA. This binding could be competed with by the natural ligands Gagp55 and NCp7 (Figure 5), but not by an unrelated RNA binding protein, the HIV-1 transactivator protein Tat (data not shown).

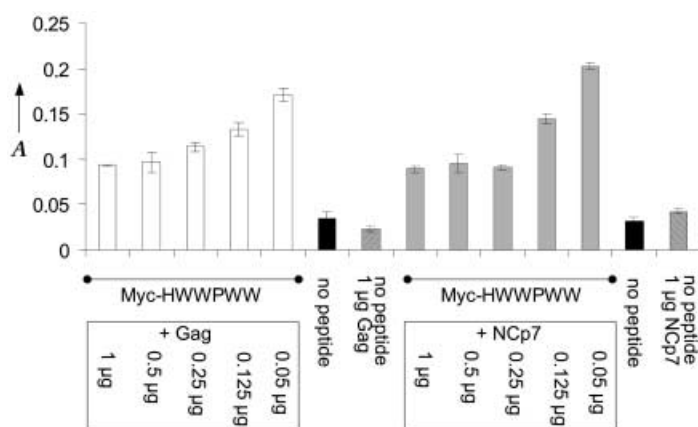


Figure 5. Binding of the myc-labeled HWWPWW peptide to full-length ψ RNA is competed with by the natural ligands Gagp55 (white bars) and NCp7 (grey bars). Black bars indicate control wells with RNA and no peptide, diagonal stripes indicate control wells without peptide but with a competitor protein. Bound peptide is detected by a horse radish peroxidase labeled anti-myc antibody.

Thus, by the phage-display approach we selected peptide ligands for RNA structures derived from the HIV-1 ψ region, and these peptides resemble the natural NCp7 ligand in terms of the binding features, including the tryptophan residues involved and the cross-reactivity with different RNA stem-loop structures derived from the ψ region. The selected peptides can now serve to derive modified peptides or small molecules with optimized binding properties to the target RNA, which could then potentially interfere with the packaging process of HIV-1 RNA genomes.

Experimental Section

Target RNAs: Full-length ψ RNA and CCR5 RNA of similar length were in vitro transcribed after PCR amplification and cloning (nucleotides 20–202 from HIV-1 pNL4-3 and nucleotides 737–890 from pcDNA3-CCR5) into pTRikan18 (Ambion). Shorter stem-loops SL1–SL3, as well as mutated stem-loops SL1–SL3, were chemically synthesized and biotinylated. All RNAs were checked on polyacrylamide gels for purity. The sequences were: SL1, biotin-TTTTTCUCGGC UUG CUG AAG CGC GCA CGG CAA GAG GCG AG; SL1 mut, biotin-TTTTTCUCGGC UUG CUG AAG CGC GCA GUC GUU-CAG GCG AG; SL2, biotin-TTTTTCGGC GAC UGG UGA GUA CGCC; SL2 mut, biotin-TTTTTCGGC GAC UAA AAA GUA CGC C; SL3, biotin-TTTTTCGGA CUA GCG GAG GCU AGU CC; SL3 mut, biotin-TTTTTCGGA CUA GCA AAA GCU AGU CC.

Screening of phage-displayed peptide libraries: RNAs (50 ng per well) in psi buffer (5 mM 2-[4-(2-hydroxyethyl)-1-piperazinyl]ethanesulfonic acid (HEPES), 100 mM KCl, (pH 7.4)) were denatured for 3 min at 95 °C and renatured for 20 min at room temperature before being immobilized on streptavidin-coated plates, either directly (SL1–SL3) or through a biotinylated primer (5'-oligo: GCTTAATACTGACGCTCTCGC, 100 pmol) complementary to the 3'-end of the ψ RNA or (3'-oligo: CCTTTAGTGAGG GTA ATT CTC G) complementary to the 5'-end of CCR5 RNA by incubating for 3 h at 4 °C. After washing, the plates were incubated with 3 different phage libraries (Biolabs) displaying peptides of 7 or 12 amino acids in a linear (7-mer, 12-mer) or a cyclic form (7-mer) for 4 h at 4 °C. After extensive washing, binding phages were eluted with glycine (100 µL, 0.2 M, (pH 2.2)) and neutralized with tris(hydroxymethyl)aminomethane (Tris)/HCl (15 µL, (pH 9.1)). After four rounds of positive selection, CCR5 RNA or mutated SL1, SL2, or SL3 RNAs were used for negative selection. Finally, phages were amplified and titered, and phage DNA was prepared for sequencing of the peptide inserts.

Peptide synthesis: All chemicals and solvents used were of analytical grade. Peptides were synthesized on an ABI 433A peptide synthesizer (Applied Biosystems, USA) by solid-phase chemistry with in situ neutralization (2 M diisopropylethylamine (DIEA) in *N*-methylpyrrolidine (NMP)) and activation with 19% *O*-(benzotriazol-1-yl)-*N,N,N'*-tetramethyluronium hexafluorophosphate (HBTU) and 7.66% 1-hydroxy-1*H*-benzotriazole (HOBt) in *N,N*-dimethylformamide (DMF) on 9-fluorenylmethoxycarbonyl-amide (Fmoc-amide) resins (Applied Biosystems, USA). After chain assembly was complete, peptides were deprotected and simultaneously cleaved from the resin by treatment with trifluoroacetic acid containing phenol (1.25%), chlorotriisopropylsilane (1.25%), 1,2-ethanedithiol (1.25%), and water (1.25%). Peptides were then lyophilized and purified by preparative HPLC. Fmoc-protected amino acids were obtained from NovaBiochem, USA. Side-chain protecting groups were as follows: Arg(Pmc), Asn(Trt), Asp(tBu), Gln(Trt), Glu(tBu), His(Trt), Lys(Boc), Ser(tBu), Thr(tBu), Trp(Boc), and Tyr(tBu), where Pmc = 2,2,5,7,8-pentamethylchromen-6-sulfonyl, Trt = trityl = triphenylmethyl, and Boc = *tert*-butoxycarbonyl.

ELISA: Streptavidin-coated plates were blocked with milk powder (3% in phosphate-buffered saline (PBS)) for 2 h at room temperature. After washing, RNAs (50 ng) from the ψ region or control RNAs were immobilized for 90 min at room temperature as described above. After washing, the amplified phage stocks (10 µL) were added for 2 h at room temperature. Binding phage were detected with mouse anti-phage antibodies conjugated with horseradish peroxidase (HRP). After addition of the HRP substrate *ortho*-phenylenediamine dihydrochloride (OPD) plates were read at 492 nm.

For peptide competition ELISA measurements, the myc-labeled HWWPWW peptide (500 ng) was added in milk powder (5% in PBS with 5 µg of yeast tRNA) to immobilized full-length ψ RNA. After washing, Gag or NCp7 protein (50 ng – 1 µg) was added for 30 min at room temperature. The bound myc-HWWPWW peptide was detected with an HRP-labeled anti-myc antibody.

Band-shift analysis: RNA (500 ng) was denatured for 5 min at 95 °C and renatured for 25 min at room temperature. The phage stock (10 µL) was added and incubated for 20 min at room temperature. Samples were run on a native polyacrylamide gel (5%) for 150 min at 75 V and 4 °C. Bands were visualized by ethidium bromide staining.

Circular dichroism spectroscopy: Spectra were obtained with a Jasco J810 spectropolarimeter (Jasco, USA) at 20 °C. The peptides had no elliptic maxima in the range of 260–290 nm, thereby allowing for direct observation of changes in the RNA spectrum with the addition of peptides. The concentration of ψ RNA was 0.2 µM and of SL3-RNA was 0.7 µM in a 100 mM potassium phosphate buffer (pH 6.5). The peptide concentrations ranged from 5–100 µM.

Acknowledgements

This work was supported by the Deutsche Forschungsgemeinschaft (SFB579 on "RNA – ligand interactions"). The following reagents were obtained through the AIDS Research and Reference Reagent Program, Division of AIDS, NIAID, National Institutes of Health: HIV-1SF2 p55 Gag (Chiron Corporation) and HIV-1MN p7 (Dr. L. Henderson). Tat protein was provided by Dr. E. Loret (France).

Keywords: HIV-1 packaging • peptides • phage display • RNA • RNA – peptide interactions

- [1] M. G. Caprara, T. W. Nilsen, *Nat. Struct. Biol.* **2000**, *7*, 831–833.
- [2] P. Mucha, A. Szyk, P. Rekowski, P. A. Weiss, P. A. Agris, *Biochemistry* **2001**, *40*, 14 191–14 199.
- [3] R. N. De Guzman, R. B. Turner, M. F. Summers, *Biopolymers* **1998**, *48*, 181–195.
- [4] J. M. Pérez-Cañadillas, G. Varani, *Curr. Opin. Struct. Biol.* **2001**, *11*, 53–58.
- [5] M. A. Weiss, N. Narayana, *Biopolymers* **1998**, *48*, 167–180.
- [6] J. R. Williamson, *Nat. Struct. Biol.* **2000**, *7*, 834–837.
- [7] N. Leulliot, G. Varani, *Biochemistry* **2001**, *40*, 7947–7956.
- [8] D. J. Patel, *Curr. Opin. Struct. Biol.* **1999**, *9*, 75–87.
- [9] A. D. Frankel, *Curr. Opin. Struct. Biol.* **2000**, *10*, 332–340.

- [10] S. D. Jayasena, *Clin. Chem.* **1999**, *45*, 1628–1650.
- [11] E. S. DeJong, B. Luy, J. P. Marino, *Curr. Top. Med. Chem.* **2002**, *2*, 289–302.
- [12] G. J. Zaman, P. J. Michiels, C. A. van Boeckel, *Drug Discov. Today* **2003**, *8*, 297–306.
- [13] H. M. E. Azzazy, W. E. Highsmith, Jr., *Clin. Biochem.* **2002**, *35*, 425–445.
- [14] I. A. Laird-Offringa, J. G. Balesco, *Methods Enzymol.* **1996**, *267*, 149–168.
- [15] J. E. Powers, M. T. Marchbank, S. L. Deutscher, *Nucleic Acids Symp. Ser.* **1995**, *33*, 240–243.
- [16] R. M. Hoet, M. Pieffers, M. H. Stassen, J. Raats, R. de Wildt, G. J. Pruijn, F. van den Hoogen, W. J. van Venrooij, *J. Immunol.* **1999**, *163*, 3304–3312.
- [17] P. F. Agris, M. T. Marchbank, W. Newman, R. Guenther, P. Ingram, J. Swallow, P. Mucha, A. Szyk, P. Rekowski, E. Peletskaya, S. L. Deutscher, *J. Protein Chem.* **1999**, *18*, 425–435.
- [18] W. J. Friesen, M. K. Darby, *Nat. Struct. Biol.* **1998**, *5*, 543–546.
- [19] W. J. Friesen, M. K. Darby, *J. Biol. Chem.* **2001**, *276*, 1968–1973.
- [20] S. Hoffmann, D. Willbold, *Biochem. Biophys. Res. Commun.* **1997**, *235*, 806–811.
- [21] G. Jonas, S. Hoffmann, D. Willbold, *J. Biomed. Sci.* **2001**, *8*, 430–436.
- [22] R. Berkowitz, J. Fisher, S. P. Goff, *Curr. Top. Microbiol. Immunol.* **1996**, *214*, 177–218.
- [23] J. Dannull, A. Surovoy, G. Jung, K. Moelling, *EMBO J.* **1994**, *13*, 1525–1533.
- [24] J. Clever, C. Sasseti, T. G. Parslow, *J. Virol.* **1995**, *69*, 2101–2109.
- [25] T. Hayashi, T. Shioda, Y. Iwakura, H. Shibuta, *Virology* **1992**, *188*, 590–599.
- [26] G. K. Amarasinghe, R. N. De Guzman, R. B. Turner, M. F. Summers, *J. Mol. Biol.* **2000**, *299*, 145–156.
- [27] G. K. Amarasinghe, J. Zhou, M. Miskimon, K. J. Chancellor, J. A. McDonald, A. G. Matthews, R. R. Miller, M. D. Rouse, M. F. Summers, *J. Mol. Biol.* **2001**, *314*, 961–970.
- [28] A. Mujeeb, T. G. Parslow, A. Zarrinpar, C. Das, T. L. James, *FEBS Lett.* **1999**, *458*, 387–392.
- [29] A. H. Maki, A. Ozarowski, A. Misra, M. A. Urbaneja, J. R. Casas-Finet, *Biochemistry* **2001**, *40*, 1403–1412.
- [30] C. Vuilleumier, E. Bombarda, N. Morellet, D. Gérard, B. P. Roques, Y. Mély, *Biochemistry* **1999**, *38*, 16 816–16 825.
- [31] N. Morellet, H. Déméné, V. Teilleux, T. Huynh-Dinh, H. de Rocquigny, M. C. Fournié-Zaluski, B. P. Roques, *J. Mol. Biol.* **1998**, *283*, 419–434.
- [32] A. C. Paoletti, M. F. Shubsda, B. S. Hudson, P. N. Borer, *Biochemistry* **2002**, *41*, 15 423–15 428.
- [33] A. Zeffman, S. Hassard, G. Varani, A. Lever, *J. Mol. Biol.* **2000**, *297*, 877–893.
- [34] J. A. Turpin, S. J. Terpening, C. A. Schaeffer, G. Yu, C. J. Glover, R. L. Felsted, E. A. Sausville, W. G. Rice, *J. Virol.* **1996**, *70*, 6180–6189.
- [35] D. R. Chadwick, A. M. L. Lever, *Gene Ther.* **2000**, *7*, 1362–1368.
- [36] R. N. De Guzman, Z. R. Wu, C. C. Stalling, L. Pappalardo, P. N. Borer, M. F. Summers, *Science* **1998**, *279*, 384–388.
- [37] L. Pappalardo, D. J. Kerwood, I. Pelczar, P. N. Borer, *J. Mol. Biol.* **1998**, *282*, 801–818.
- [38] M. F. Shubsda, A. C. Paoletti, B. S. Hudson, P. N. Borer, *Biochemistry* **2002**, *41*, 5276–5282.

Received: June 2, 2003 [Z 681]